scientific reports

Check for updates

OPEN

Reducing uncertainties of climate projections on solar energy resources in Brazil

Francisco José Lopes de Lima[1,3], André Rodrigues Gonçalves[1], Rodrigo Santos Costa[1], Marcelo Pizzuti Pes[1,3], Ana Paula Paes dos Santos[1], Jose Antonio Marengo Orsini[2,4,5], Enio Bueno Pereira[1] & Fernando Ramos Martins[3]✉

The share of solar power in Brazil's electrical grid has rapidly increased, relieving GHG emissions and diversifying energy sources for greater energy security. Besides that, solar resource is susceptible to climate change, adding uncertainty to electrical grid resilience. This study uses satellite and reanalysis data to evaluate the performance of CMIP6 models in replicating and predicting surface solar irradiance (SSR) in Brazil. The results from the most reliable models indicate an increase in SSR by 2% to 8% in most regions, with a decrease of around 3% in the South. These findings highlight the potential for increased photovoltaic (PV) yield if backed by supportive public policies while underlining the importance of uncertainty assessment of climate models.

Solar energy is a promising alternative to meet the growing electricity demand while reducing greenhouse gas emissions. However, they are weather-dependent and require careful planning to minimize the impact of the intrinsic intermittence on the energy distribution system[1]. Several worldwide studies investigated the time and spatial variability and tendency of weather and climate-driven renewable energy resources based on data provided by climate models[2–7]. Solar radiation assessments based on climate models found an average decrease of 0.1 to 0.4 W/mÂ² per decade from 1979 to 2014 globally[8]. Several studies for Europe show that PV power generation will increase at the end of the century[2,5,6] despite some evidence that the future climate scenarios can drive a more complex spatial change of surface solar radiation (SSR)[9]. Nevertheless, other studies adopting a small subset of models or even downscaled high-resolution climate projections point in the opposite direction, indicating a decrease in PV potential for Northern European countries by the end of the century[10,11]. In summary, previous studies suggested that the uncertainty endures showing distinct climate change signals depending on the methodological approach used in investigation[2,10,12].

Since 2018, Brazil has been witnessing a significant surge in its installed PV capacity, which has now surpassed 30.7 GW in the second quarter of 2023[13–15]. As PV power generation is set to play a more substantial role in Brazil's future energy mix, it becomes imperative to delve into the impact of climate change on the spatial and temporal variability of solar energy.

It's worth noting that more assessment studies need to be conducted that specifically address the impact of climate on solar radiation over Brazilian territory. For instance, historical records of surface solar irradiance at 129 automated weather stations have shown both positive ($+40 Wh/m^2$ per year) and negative ($-50 Wh/m^2$ per year) trends for the northern and southern portions of the Brazilian Northeastern (NEB), respectively[16]. Recent studies based on global climate models have indicated an increase in solar energy potential for most of Brazil, with a high level of resilience for a 4-degree specific warming level scenario[17,18]. However, these results also present conflicting outcomes for Brazil's Southeast and Midwest regions, suggesting high uncertainty. Zuluaga *et al.* showed that PV power generation in Brazilian territory would likely decrease by the end of the century in both SSP2-4.5 and SSP5-8.5 scenarios, except for the northern Amazon region[19] based on an ensemble from the CMIP6 climate models.

The previous results revealed a high level of uncertainty in climate change impact assessments, partly due to the different methodologies and datasets adopted. A more rigorous selection of the climate models to be used in an ensemble analysis, focusing on selecting those with the best performance and ability to represent current

[1]Division of Impacts, Adaptation and Vulnerabilities, Brazilian Institute for Space Research, São José dos Campos, SP 12227-010, Brazil. [2]National Center for Monitoring and Early Warning of Natural Disasters, São José dos Campos 12247-016, Brazil. [3]Institute of Marine Science, Federal University of São Paulo - campus Baixada Santista, Santos, SP 11070-102, Brazil. [4] Graduate Program in Natural Disasters, UNESP/CEMADEN, São José dos Campos, Brazil. [5]Graduate School of International Studies, Korea University, Seoul, South Korea. ✉email: fernando.martins@unifesp.br

climate patterns, is essential in improving the analysis of future climate scenarios. Bias-correction methods and statistical indicators to evaluate the model's skill in reproducing spatial and seasonal patterns observed in historical reference datasets, like satellite-based or meteorological reanalysis, are fundamental to achieving more confidence in the climate change impact assessment.

This work aims to reduce uncertainties in the future surface solar irradiance SSR and PV yield for Brazilian territory by departing from an accurate historical dataset combining satellite and reanalysis and adopting reliable statistical methods to rank the CMIP6 climate models regarding their ability to represent spatiotemporal variability of SSR. We used the ensemble with the highest-skill CMIP6 models to assess the impact of climate change on solar energy up to 2100 under SSP2-4.5 and SSP5-8.5 scenarios in order to support energy entrepreneurs, governmental and non-governmental organizations in planning and building the Brazilian power generation system resilient to future climate conditions. Case studies for nine particular interesting sites for PV power generation delivered geographical outcomes that can help design and develop public policies to promote environmental sustainability and social energy justice. All research results and Python codes developed for data analysis are available for public access[20,21].

Results

Figure 1 provides a comprehensive view of the performance of CMIP6 models in reproducing SSR spatial patterns, providing visual information on the alternation between positive and negative bias for Brazilian territory. Uncertainty in model estimates is noticeable due to the large spread of deviations. The 40-models' ensemble (ENS) reproduces the SSR's spatial pattern over Brazilian Northeast and Central regions with reduced bias. Nevertheless, the ENS overestimates (around $50W/m^2$) the climatological SSR in the Amazon region. These results agree with findings showing a negative bias for precipitation outputs of CMIP6 models for the north of the Amazon[22–24].

Figure S1 in the Supplementary Material shows the bias-adjusted reanalysis ($ERA5_{QM}$) for the 1980-2014 period used as the reference dataset to evaluate CMIP6 models' skill in representing spatial and seasonal patterns in three target regions (see Fig. 2): Brazilian Northeast (area A1), South (area A2) and Central (area A3). Regarding the target area A1, model M2 overestimates the SSR around $40W/m^2 - 50W/m^2 (\approx 15\% - 20\%)$ while M5, M18, M26, and M34 underestimate by the same amount. Most models overestimate around $30W/m^2$ $(\approx 12\%)$ in areas A2 and A3, while models M5, M6, and M31 underestimate up to $20W/m^2 (\ 8\%)$.

The results of the spatial correlation between CMIP6 outputs and $ERA5_{QM}$ are available in the supplementary material (Table S1) that delivers information on the monthly spatial correlation presenting statistical significance (p-values < 0.05) achieved by climate models in the three target areas. The ensemble (ENS) and twenty-two CMIP6 models presented a significant positive correlation $(p < 0.05)$ in all twelve months for all three target areas. The ENS presented the best correlation index in the three target areas, supporting the benefit of working with model ensembles. The other eighteen models presented no significant correlation, mostly in transition months between wet and dry seasons (April and October), and were discarded for the following analysis.

In the next step, the Taylor Skill Score (TSS) (described in $eq.2$) was used to determine how accurately the twenty-two CMIP6 models depict the seasonal changes in SSR within the three target areas. Figure 3 displays the Taylor diagram and Table S2 (Supplementary Material) lists the time correlation index (r), unbiased root mean square deviation ($uRMSD$), and standard deviation (SD) ratio attained by the 22 models and the ENS, assuming the $ERA5_{QM}$ dataset as a reference. Time correlation was computed over the twelve-month climatological cycle. The blue markers denote the ten models presenting TSS greater than 0.9.

A second ensemble (referred to as SME) was processed using the ten best-performing CMIP6 models. The statistical parameters achieved by SME in the three target areas are also listed in Table S2. The SME showed a little higher standard deviation ratio than the ensemble ENS with all 40 CMIP6 models; however, it overcomes the ENS in all other metrics, including the TSS (0.96 compared to 0.90). The maps shown in Fig. 2 indicate around 20% reduction in the standard deviation of the SSR data from the SME compared to the ENS in the whole Brazilian territory. The dispersion among members is related to the uncertainty in the ensemble mean, evidencing that the SME attained an expressive reduction in uncertainty while sustaining similar skill in reproducing SSR historical climatology.

Model M25 (HadGEM3-C31) is the top-performing model in terms of TSS, with the highest time correlation and lowest $uRMSD$. The ENS has the second lowest (SD) but performs poorly in other statistical indexes compared to the ten best-performing models.

The SSR changes for future scenarios obtained from SME are presented in three timeslices: near-future (2015-2040), mid-term future (2041-2070), and end-of-century (2071-2100). Complete plots and maps for the three timeslices and both climate scenarios (SSP2.45 and SSP5.85) are available at https://doi.org/10.6084/m9.figshare.25396612 for public access.

Figure 4 shows the seasonal variation of the climate change factor (CCF) and SSR in the three target areas. More details on seasonal variation of SSR derived from the $ERA5_{QM}$ and CMIP6 Smart Ensemble (SME) are shown in Figs. S3 to S5. In Brazilian Northeast (Area A1), Fig. 4b shows that CCF is positive throughout the year, except in January and February for the end-of-century. In both climate scenarios, the highest CCF occurs in transition periods between dry and wet seasons, September to November and March to April. Due to the CCF seasonal variation, the monthly mean SSR increases around $10W/m^2$ in the austral autumn and spring seasons in both scenarios and all timeslices. Such an increase in SSR agrees with the reduction in precipitation, notably for the SSP5-8.5 scenario[25]. The seasonal CCF variation for the central region of Brazil (area A3, Fig. 4d) is similar to area A1. The CCF assumes positive values throughout the year, with the highest $CCFs$ in the wet season from October to March (3-5% in SSP5-8.5 and 2-3% in SSP2-4.5) at the 2071-2100 timeslice.

Figure 4c shows an opposite seasonal pattern in the South of Brazil (area A2). The CCF shows negative values most of the year except for January and February, ranging from 0.5 to 1.5% in both scenarios and

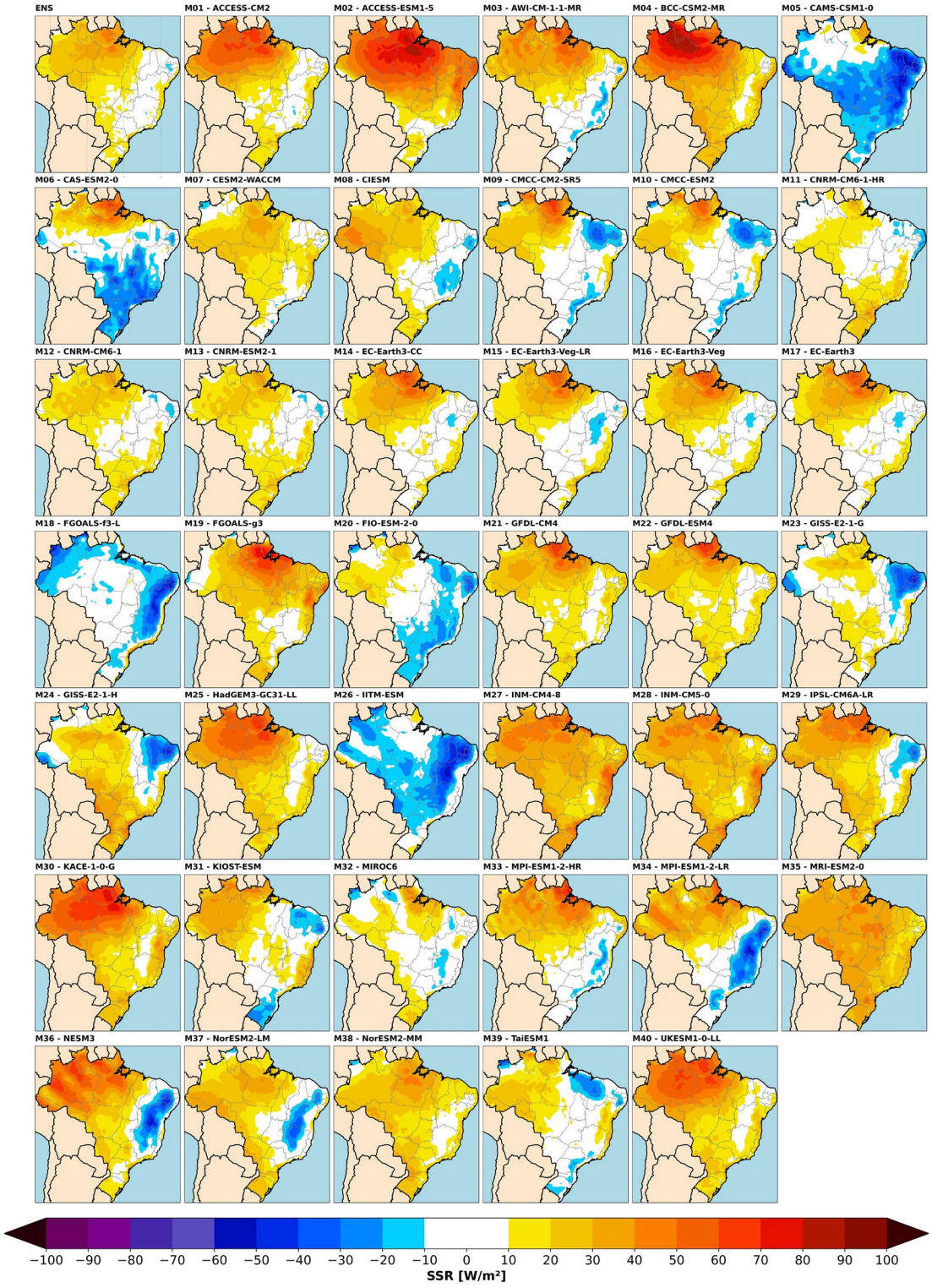

Fig. 1. The panel presents the mapping of the BIAS deviation (in W/m^2) shown by the SSR estimates provided by the ensemble (upper left corner) and by each of the forty climate models from CMIP6 used in the study. The model names are positioned above the corresponding map. The authors prepared maps using the available Python libraries.

timeslices. The decrease in SSR is more severe during the Wet-Dry transition months when the predicted CCF is around-2.0% (-4.5%) in SSP2-4.5 (SSP5-8.5) at the end-of-century.

Figure 5 displays seasonal maps of the CCF for the Brazilian territory according to SME. For the near-future timeslice (Fig. 5a and d), the impacts are quite similar in both scenarios (SSP2.45 and SSP5.85). The SSR

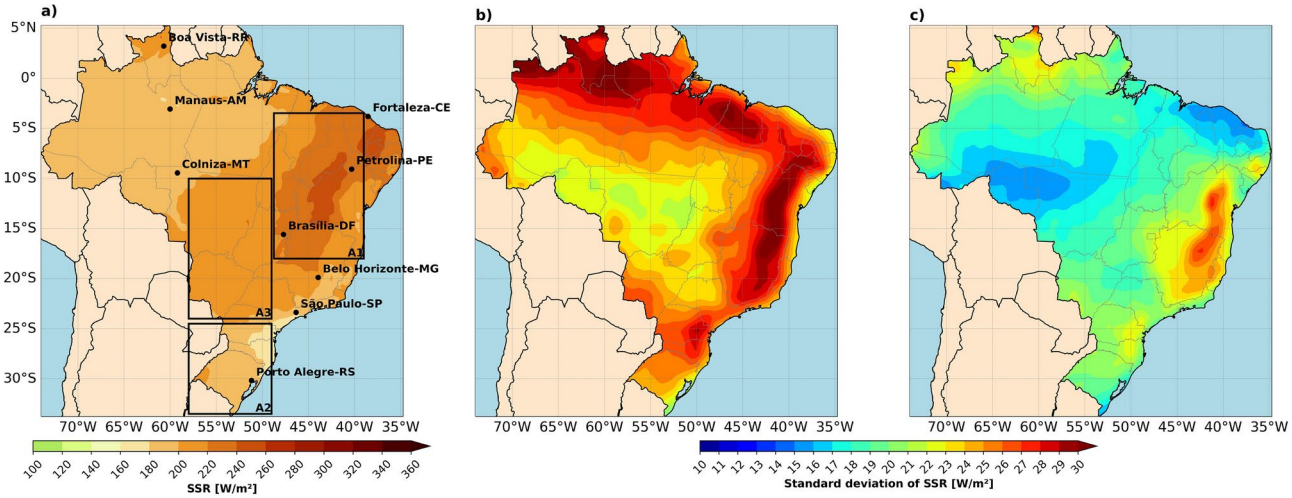

Fig. 2. (left) Surface solar irradiance SSR reference map based on the $ERA5_{QM}$. The rectangles indicate the target regions used in the performance evaluation of CMIP6 models: area A1 in the Northeast, A2 in the South, and A3 in Central Brazil. Standard deviation maps of SSR calculated among members of the ENS (central) and SME (right). The authors prepared maps using the available Python libraries.

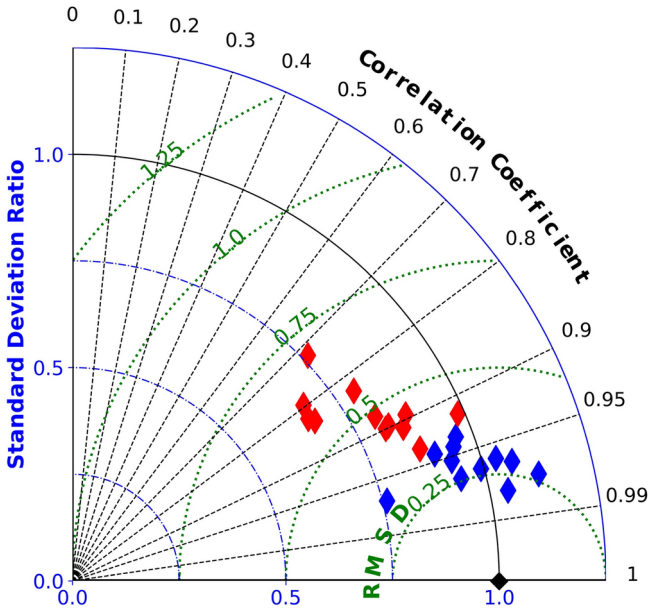

Fig. 3. Taylor's diagram compares the CMIP6 model's performance regarding the $ERA5_{QM}$ database. Each marker represents the statistical metrics achieved by the CMIP6 climate models and the ENS ensemble. The blue (red) markers indicate the CMIP6 climate models with a Taylor index TSS above (below) 0.9. The black marker indicates the statistical metrics achieved by ($ERA5_{QM}$). Table S2 (Supplementary Material) lists the statistical metrics achieved by each model and ensemble.

is expected to increase by up to 3% in the Amazon and up to 5% in Central and Southeastern Brazil, though more pronounced during Spring and Summer. The 2070-2100 timeslice (Fig. 5c and f) shows a decrease of up to -2% (-4%) in SSR in the northern part of the Brazilian Northeastern region under SSP2-4.5 (SSP5-8.5) during Summer. An SSR decrease of up to 5% is also noticed in Southern Brazil for SSP5.85, lingering from Fall to Spring. On the other hand, SSR is likely to increase by up to 6% (10%) in the Amazon, Central, and Southeastern Brazilian regions under SSP2-4.5 (SSP5-8.5).

Figure 5 shows a noticeable signal in the annual average maps with CCF ranging from 2% to 6% in the near future (SSP2-4.5) to -3% to 8% by the end of the century in SSP5-8.5. Those amplified positive signals in CCF during spring over semi-arid and Central regions of Brazil play a crucial role in reducing the vulnerability of the Brazilian electrical system to climate change, especially where most of the utility-scale PV power plants are currently operating. The Brazilian Interconnected Electricity System (SIN) mainly relies on hydropower

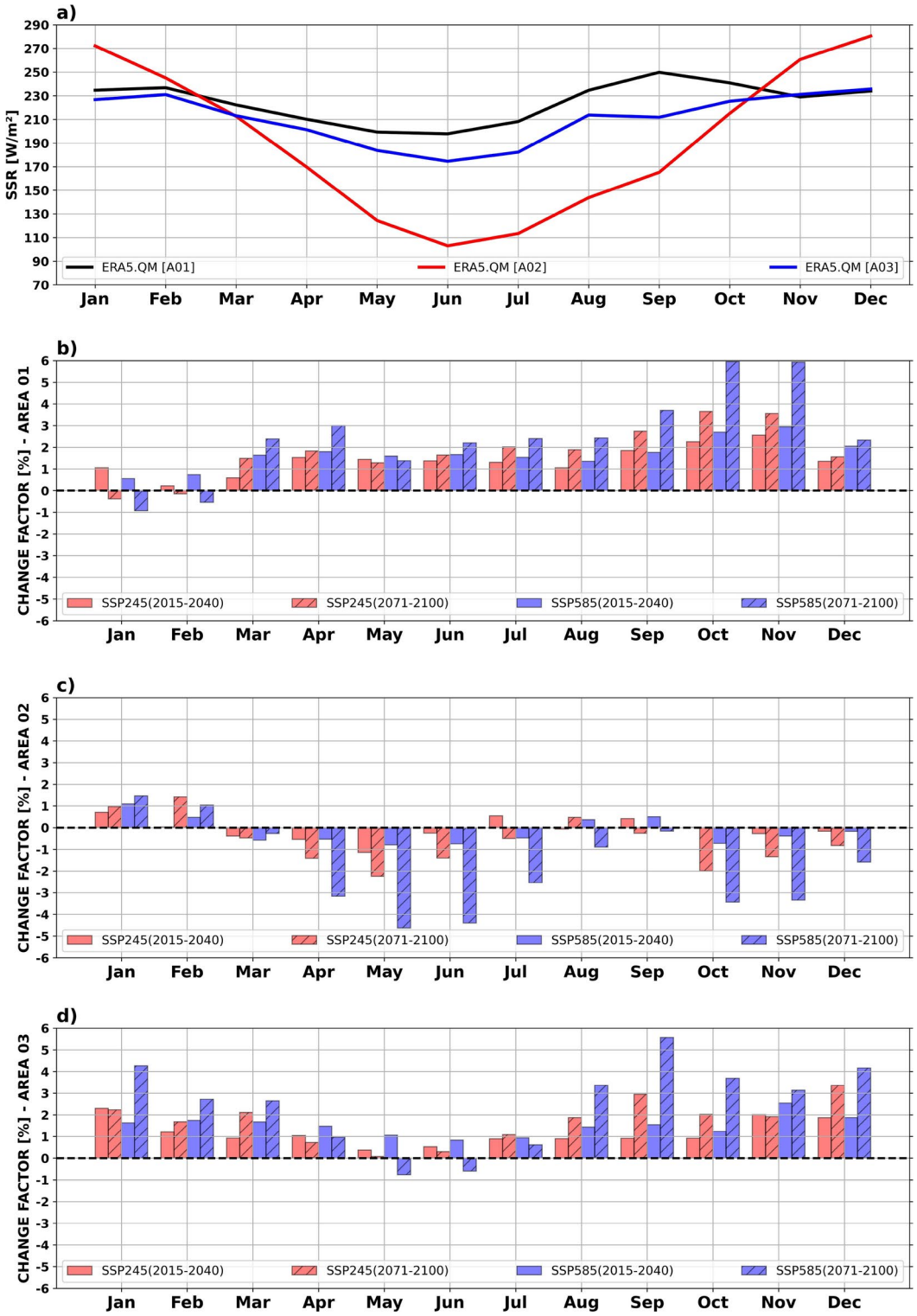

Fig. 4. (**a**) Seasonal variation of mean (SSR) based on the $ERA5_{QM}$ database; (**b**) Seasonal variation of mean CCF obtained from SME for SSP2-4.5 and SSP5-8.5 pathways for target area A1; (**c**) for area A2 and; (**d**) for area A3.

and faces critical operation from September to November due to the end of the dry season. During these months, hydropower reservoirs are usually depleted and exposed to climate variability, implying high risks. Past electricity supply crises are clear evidence of this situation[26]. In this sense, the higher solar resource levels during spring add resilience to the future of the national electricity system for both scenarios. However, impacts on

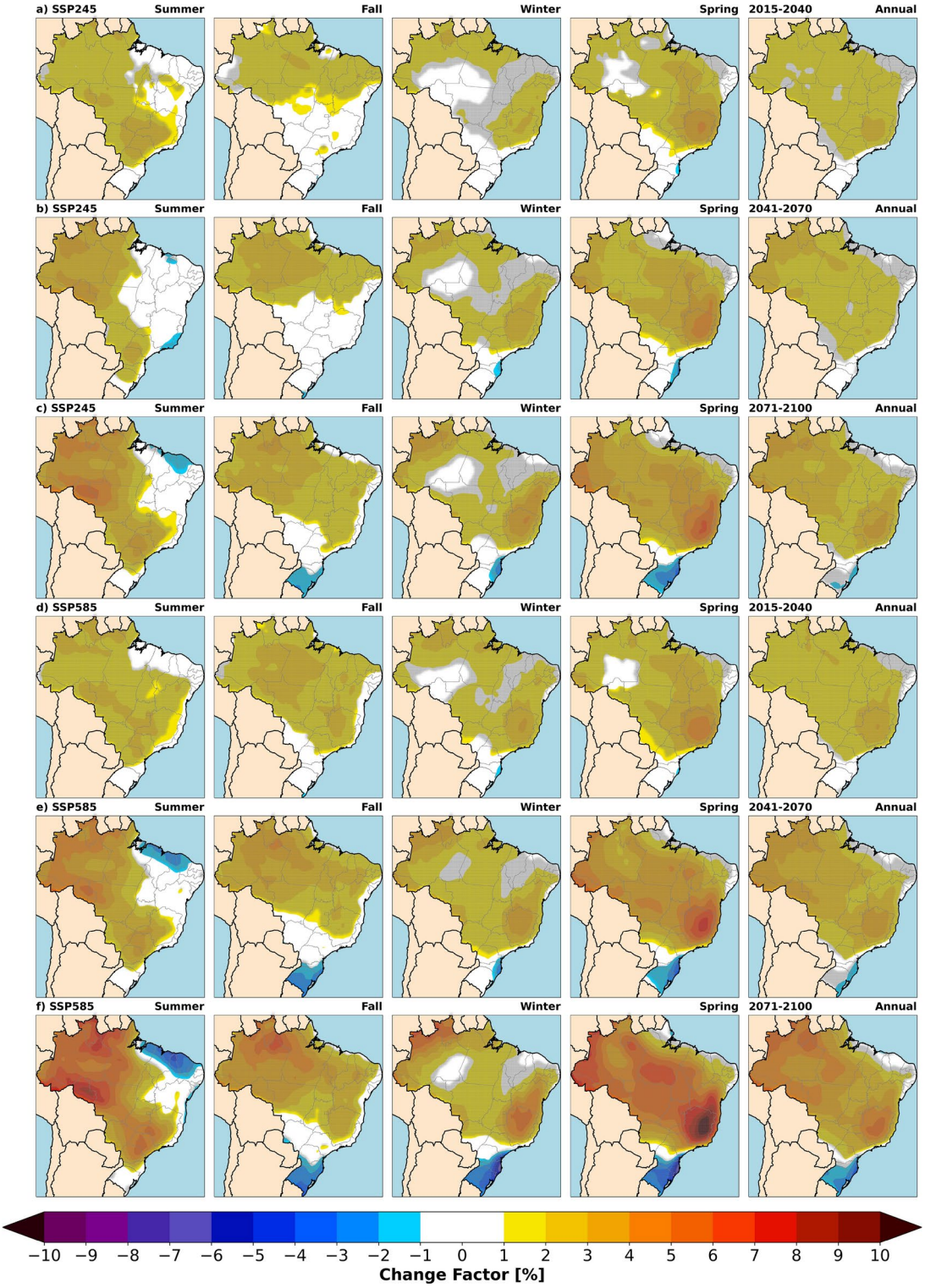

Fig. 5. The seasonal mean CCF predicted by the SME for the SSP2-4.5 in 2015-2040 (**a**), 2041-2070 (**b**), and 2071-2100 (**c**) timeslices; and for SSP5-8.5 in 2015-2040 (**d**), 2041-2070 (**e**) and 2071-2100 (**f**) timeslices. The columns are from left to right: summer, autumn, winter, spring, and annual. The gray dots over the maps represent the grid locations with statistical significance (p-value <0.05). The authors prepared maps using the available Python libraries.

other renewable resources (wind, hydro) are also expected, and an integrated evaluation should be conducted in the work in progress.

Case studies for metropolitan and remote areas

Solar PV technologies have rapidly grown in Brazilian metropolitan regions (MR) due to a sharp cost reduction and recent regulations encouraging distributed generation[13]. The SSR's spatial distribution and future trends highlight the challenges in optimizing solar power benefits for Brazil's energy mix while reducing risks and GHG emissions to fulfill international commitments. Based on recent works using data from PV power systems operating in Brazil[27], we used the performance ratio (PR) around 0.8 to evaluate the impact of climate change on solar PV yield.

Figure 6 shows the annual PV yield from 1980 to 2100 assessed using the SSR outcomes of the SME for SSP2-4.5 and SSP5-8.5 pathways in seven MRs and two remote areas, covering different climate regimes. We assumed that technological advancements in PV technology will offset the losses in solar energy conversion due to the rise in ambient temperature. Table 1 lists the trend slope and p-value of the linear regression fitted for the nine locations and climate pathways. The statistically significant trends are highlighted in bold blue numbers.

Fortaleza and Petrolina are MRs located in the Northeastern region of Brazil, where SSR is at its highest. Fortaleza is on the coast near the Equator and holds more than three million inhabitants. It also has abundant wind energy resources throughout the year[28,29], which allows hybrid wind-solar projects to take place, reducing power intermittence. On the other hand, Petrolina is located in the semiarid region close to the largest regional hydropower reservoir, Sobradinho (1050 GW), where floating PV power plants could improve water storage and management during extreme drought periods and meet water demands for other uses besides power generation[30,31].

Based on Fig. 6, the SME predicts that PV yield will increase $0.11 kWh/kW_p$ per year ($0.18 kWh/kW_p$ per year) in Petrolina, until the end of the century for SSP2-4.5 (SSP5-8.5) pathway (with low statistical significance). However, SME predicts a significant negative trend ($-0.25 kWh/kW_p.y^{-1}$ ($-0.36 kWh/kW_p.y^{-1}$)) on annual PV yield for the same climate scenarios in Fortaleza. Although the results indicate a likely reduction in solar PV resources on the equatorial coast of the Brazilian Northeast, the portfolio is rather resilient since most large-scale PV utilities are being implemented in the semi-arid region. The impacts are limited to $+/-2\%$ over the current PV yield (reference timeslice) and may not primarily affect the financial feasibility of the sector.

Brasilia and Belo Horizonte are important MRs where solar power rapidly expands due to the region's abundant solar resources, and reduced seasonal variation. Recent studies indicate that investments in PV power distributed generation (PVDG) have the lowest payback period in Brazil[32]. For both climate scenarios, the SME projections show a positive trend of PV systems yield in both areas in the upcoming years. However, the trend slope is around twice as high in SSP5-8.5 (0.46 to $0.66 kWh/kW_p.y^{-1}$). It means around a 5% increase in SSR in the more extreme scenario.

São Paulo is the largest Brazilian MR, with nearly 22 million inhabitants living in around $8000 km^2$ in the Brazil Southeast. São Paulo is the country's primary energy consumption center and has seen an exponential increase in PVDG since 2020[13,14]. Figure 6 and Table 1 indicate that climate change will not particularly affect the annual PV yield as the trend slope is slight and has no statistical significance.

Porto Alegre is in the Brazilian Southern region, where SSR has the highest seasonal variability due to the solar geometry and climate dynamics in the region[33–35]. The SME predicts a robust decreasing trend up to -3% around $-40 kWh/kW_p.y^{-1}$ under SSP5-8.5 for Porto Alegre. The decreasing trend is also present under SSP2-4.5 but is not statistically significant. However, the South of Brazil also has a high wind energy potential[29], and hybrid wind-solar power projects can be an alternative to reduce the impact of climate change in future solar PV generation.

The three remaining locations, Manaus, Boa Vista, and Colniza, are facing a pressing issue of energy access. Despite being far from the leading consumer centers, these regions urgently need to address their energy challenges. Manaus, the largest urban center in the Brazilian Amazon region, is a hub of economic activity. Boa Vista, the northernmost state capital in Brazil, is not served by the National Interconnected Electricity System (SIN). Still, diesel-powered thermal generation mainly meets its electricity demand, with a small fraction imported from neighboring countries. Colniza, a small town in the southern Amazon region, has an economy heavily based on agriculture, with a large portion of the population living in rural areas without access to electricity utilities.

Most of the Amazon region is not linked with the Brazilian Interconnected Electricity Distribution System (SIN). Instead, isolated power systems that rely on fossil fuels are spread throughout the region, and their costs are financed by compulsory taxes included in the energy tariff paid by all Brazilian electricity consumers. Solar PV systems are the primary alternative for isolated power systems to reduce greenhouse gas emissions and lower high taxes on electricity bills. According to the SME outcomes, the PV yield scenarios show the highest increasing trend in the Brazilian Amazon region for both SSP pathways. In the SSP5-8.5 scenario, the PV yield may increase up to 4%, strengthening the solar power option to meet the power demand in the region.

Conclusions

This study shows that future climate projections present significant uncertainties, introduced not only by scenarios and assumptions but mainly by the spread of climate models' performance. Results show that uncertainties are significantly reduced by choosing an appropriate subset of best-performing models while maintaining skill in simulating SSR patterns. In general, the CMIP6 models tend to overestimate SSR in the Amazon, agreeing with other assessments showing a decrease in precipitation in this region[22,23] while performing better in Brazil's Northeast region. Future projections show an increase in SSR by 2% to 8% in most Brazilian regions, with a decrease of around 3% in the South, particularly under the SSP5-8.5 scenario. The SSR change signal

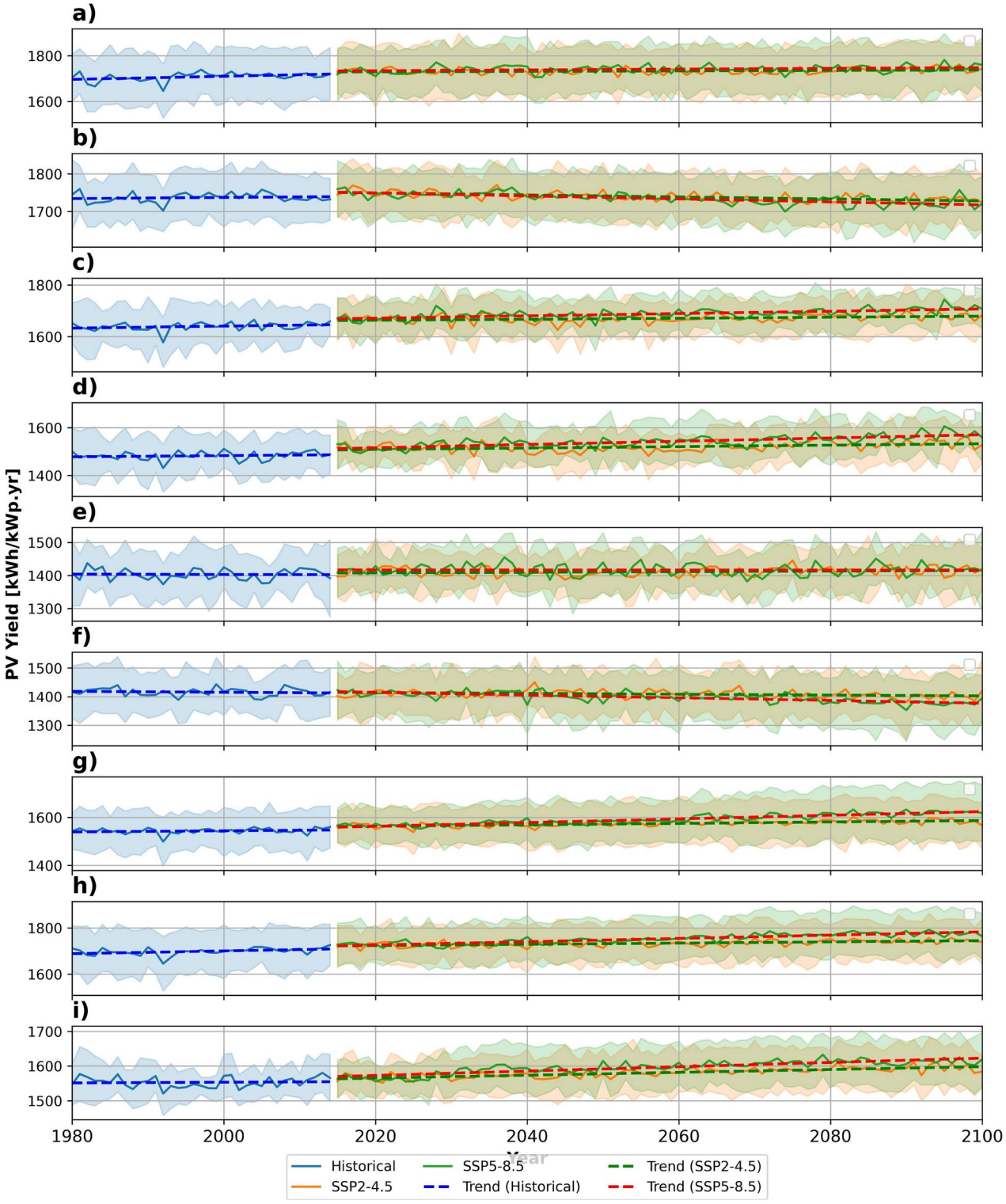

Fig. 6. Annual trends of SSR generated from SME outputs for seven metropolitan areas of Brazil - (**a**) Petrolina, (**b**) Fortaleza, (**c**) Brasília, (**d**) Belo Horizonte, (**e**) São Paulo, (**f**) Porto Alegre and (**g**) Manaus - and two remote areas (**h**) Boa Vista (located further north in the Brazilian Amazon), and (**i**) Colniza (located in the deforestation belt in the Southern Amazon). The geographical location of the nine spots is shown in Fig. 2.

Location	Historical timeframe		SSP2-4.5		SSP5-8.5	
	Trend $kWh/kW_p.y^{-1}$	p-value	Trend $kWh/kW_p.y^{-1}$	p-value	Trend $kWh/kW_p.y^{-1}$	p-value
Petrolina	0.65	0.25	0.11	0.44	0.18	0.22
Fortaleza	0.19	0.58	**− 0.25**	**0.01**	**− 0.36**	**0.00**
Brasília	0.37	0.39	**0.20**	**0.05**	**0.46**	**0.00**
Belo Horizonte	0.23	0.64	**0.28**	**0.02**	**0.66**	**0.00**
São Paulo	0.0 1	0.98	0.09	0.33	0.03	0.75
Porto Alegre	− 0.18	0.66	− 0.15	0.17	**-0.49**	**0.00**
Manaus	0.24	0.59	**0.29**	**0.01**	**0.73**	**0.00**
Boa Vista	0.61	0.73	**0.27**	**0.03**	**0.77**	**0.00**
Colniza	0.10	0.25	**0.40**	**0.00**	**0.63**	**0.00**

Table 1. The trend for PV yield and the corresponding p-value from time series for nine locations with diverse SSR climatology based on predictions for two scenarios, SSP2-4.5 and SSP5-8.5. Significant p-values at 5% are highlighted in bold.

over the Brazilian Northeastern region matches with other studies[18,19,24]. However, for central and southeast Brazil, results vary depending on the methods and models adopted, evidencing the higher uncertainty. The low magnitude of changes compared to model ensemble spread remains as the main source of uncertainty and is an inherent limitation of this study. Nevertheless, this approach improves the confidence on climate change impact over SSR due to a broad and systematic assessment of a large sample of models.

Higher SSR levels were significant in the trend analysis for most Brazilian metropolitan areas. Moreover, the seasonal change depicts an increased SSR during Brazilian drier months (from September to November), reducing the vulnerability of Brazil's electrical system, which relies heavily on hydropower. The results also indicate a trend of increased PV generation productivity for future climate scenarios across much of Brazilian territory, with a more pronounced impact in the Amazon region that is not served by the National Interconnected Electricity System (SIN). However, in some areas, climate models point to a decrease in productivity of less than -3% along the northeastern coast and the southern part of the country by the end of the century. From an energy planning perspective, these results may support regional development strategies for improving the resilience of the Brazilian power system to future climate conditions. More studies investigating changes in the frequency of SSR extremes could contribute to a more complete assessment, inviting further research and engagement.

Methods

The study area comprises continental Brazilian territory, the fifth-largest country in the world. From North to South, Brazil extends for almost 4400 km, with the Equator and the Tropic of Capricorn running through it. Most of the population lives near the Atlantic coast, and the largest cities are in the Southeastern region. Brazil encompasses diverse important biomes, including the Amazon Forest in the North region, Pantanal wetland in the Mid-west area, Caatinga (semiarid) in the Northeast, and Pampa in the South.

Despite the diverse climate and environmental features[33,35], previous studies indicated that surface solar irradiation is relatively uniform in Brazilian territory[36]. The semi-arid area of the Northeastern Brazilian region receives the highest incoming solar irradiation, up to 6.27 $kWh.m^{-2}.day^{-1}$). The SSR is around 6.0 $kWh.m^{-2}.day^{-1}$ in Brazil's Northern and Central regions during the dry season from July to September. The Southern and Southeastern coastal regions present higher annual variability due to the higher latitude, the onset of the monsoon system during summer, and the higher frequency of cold fronts during the fall and winter. South Brazil receives higher SSR than the Northern region during the austral summer due to the more extended day length and higher cloud coverage in the North linked to the southern shift of the Intertropical Convergence Zone (ITCZ).

Data analysis procedure

Figure 7 illustrates the analytical steps for assessing the impacts of climate change on the solar energy resource in Brazilian territory. The investigation used SSR data from three repositories: the Coupled Model Intercomparison Project Phase 6 (CMIP6), the ERA5 reanalysis provided by ECMWF (European Centre for Medium-Range Weather Forecasts), and satellite-based data provided by INPE (Brazilian Institute for Space Research).

The CMIP6 provided the SSR data from 40 global climate models. Before using CMIP6 future projections, we assessed each model's reliability by comparing them with a truth reference for spatiotemporal patterns. Several studies suggest that the ERA5 reanalysis database fulfills the required features (long and continuous time coverage, spatially homogeneous, and reliable ground data assimilation) to be the truth reference database[22,34]. However, the ERA5 overestimates the SSR throughout Brazilian territory due to limitations in its numerical radiative parameterization like aerosol optical depth (AOD) due to biomass burning events in the Amazon and Central area of Brazil during the dry season and sub-grid shallow clouds that prevails in the tropical humid atmosphere over the continent[37–39].

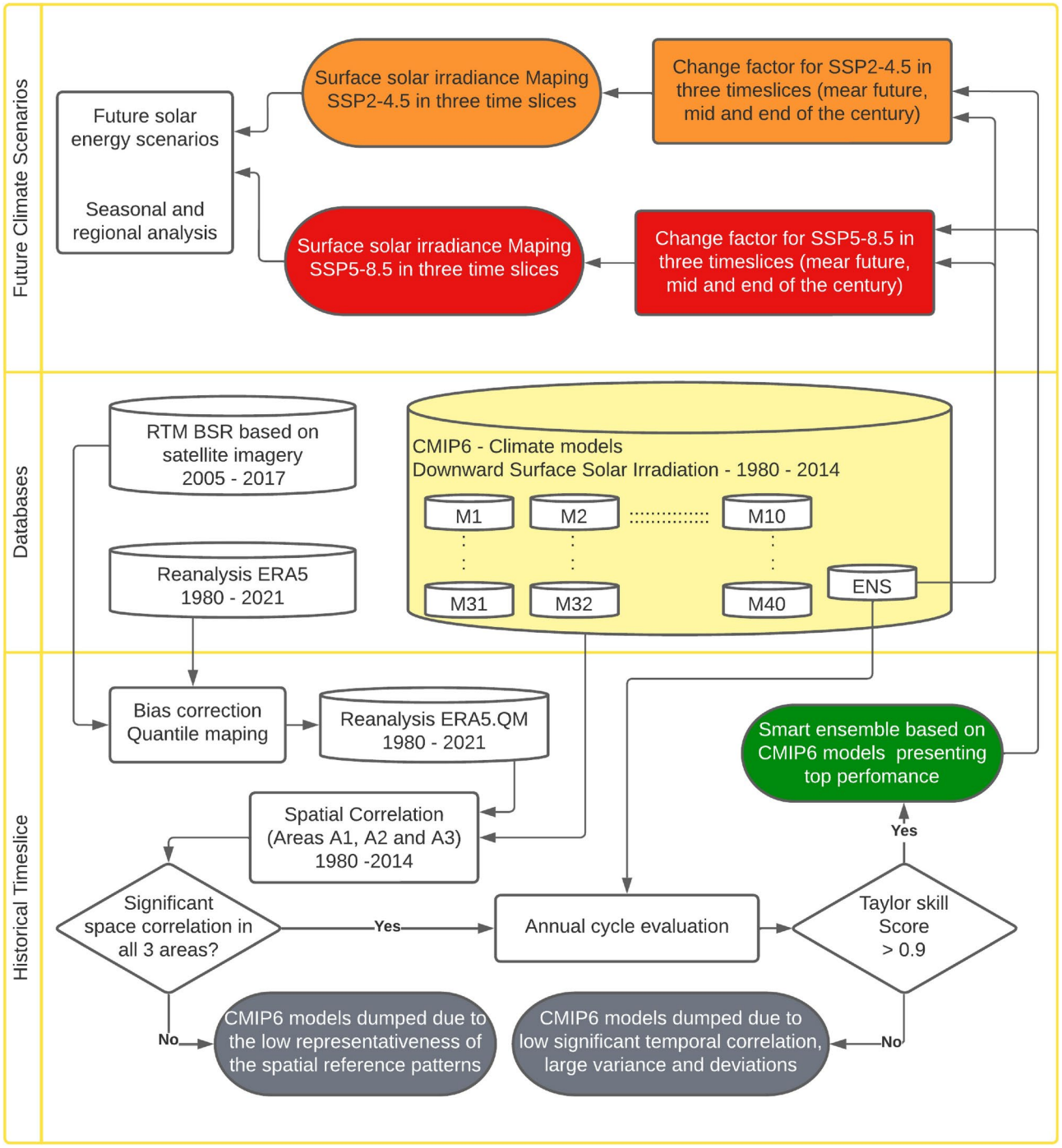

Fig. 7. The flowchart shows the step sequence of the methodology used to investigate future solar energy resource scenarios based on CMIP6 climate models.

Solar radiation databases

BSR database

The BSR database comes from the radiative transfer model BRASIL-SR, a semi-empirical model based on the two-stream approach to solve the radiative transfer equation in the atmosphere using cloudiness data obtained from GOES-East satellite imagery[37]. Previous studies comparing the BSR database and ground data revealed low uncertainties for monthly averages of the daily downward surface solar irradiation. The root mean squared error (*RMSE*) obtained for monthly averages were around 4% and 12% depending on the climate season (dry or wet) and environmental conditions like atmospheric aerosol load, land use, and others[40]. The BSR database is available at http://labren.ccst.inpe.br/atlas_2017-en.html or by contacting the research team. This study used daily averages of global downward surface solar irradiance (SSR) provided by the model BRASIL-SR from 2005 to 2017 at a spatial resolution of 0.03° x 0.05° (around 4 km x 4 km).

ERA5 reanalysis data

The ERA5 reanalysis dataset is based on the Integrated Forecasting System (IFS) Cy41r2, which uses a 4D-Var observational data assimilation scheme. The ERA5 data are available on the Copernicus Climate Change Service Data Store - CDS web platform https://cds.climate.copernicus.eu/cdsapp#!/dataset/[41] in hourly time steps with a spatial resolution of 0.25° ($\approx$27 km). This study used the daily integrated downward surface solar irradiation data (identified as $SSRD$ in the output variable list) between 1980 and 2014 (34 years) for the entire Brazilian territory. Previous study[42] demonstrated that ERA5 performed well for the Brazilian territory, particularly in Brasília, Petrolina, and FlorianÃ³polis ground measurement sites.

CMIP6 database

The CMIP6 database includes the climate models' outputs for the historical timeframe (1850-2014) and future periods: 2025-2040 ("near future"), 2040-2070 ("mid of the century"), and 2070-2100 ("end of the century") based on updated emissions scenarios[43,44]. The climate predictions are related to the RCPs (Representative Concentration Pathway) denoting a greenhouse gas concentration (not emissions) trajectory adopted by the IPCC, and the Shared Socioeconomic Pathways (SSPs), which describe projected socioeconomic global changes up to 2100 regarding the different mitigation and adaptation strategies to climate changes impacts.

This work encompasses two future scenarios, the SSP2-4.5 and SSP5-8.5. Both SSP2 and SSP5 scenarios assume a delay in global cooperation and were chosen due to the higher energy demands at the end of the century[45]. The SSP2 is the "middle of the road" pathway in which the global population growth is moderate, challenges to reducing vulnerability to societal and environmental changes remain, and energy use intensity declines after 2040. The SSP2-4.5 is the most probable scenario considering the current trajectory and the exhaustible character of non-renewable fuels, presenting intermediate challenges for mitigation[46].

The SSP5 is the "fossil fuel development" scenario with increasing inequalities and stratification across and within countries, and the economic and social development is based on energy-intensive lifestyles linked to the abundant exploitation of fossil fuel resources around the world. In SSP5-8.5, emissions continue to rise throughout the 21st century, and it is generally considered the basis for worst-case climate change scenarios due to the higher mitigation challenges[47]. For Brazil, SSP2 implies GDP and population peaking around 2050, pressing for higher energy demand, while SSP5 relies mainly on fossil fuels[48].

Table 2 lists the forty CMIP6 climate models (GCM) used in the study. The table also provides the spatial resolution of each model. The criteria for model inclusion was the data availability of monthly Surface Downwelling Shortwave Radiation (SDSR) with a spatial resolution of up to 250 km. The CMIP6 data was downloaded from https://esgf-node.llnl.gov/search/cmip6/. We used only the first member (realization1) of each GCM.

ERA5 bias correction

Satellite-based SSR products have shorter time series than meteorological reanalysis but present better accuracy[42]. Previous studies show that the BSR time-series presents low bias throughout the Brazilian territory[40]. Nevertheless, its time coverage is shorter than required to serve as reference data for the performance evaluation of CMIP6 historical simulations. In order to meet the time coverage and confidence required for the reference database, we used a bias correction method for the ERA5 database, assuming the BSR database as the reference truth. The Quantile Mapping (QM) method[49,50] consists of a numerical transformation of the ERA5 surface solar irradiation (SSR_{ERA5}) database such that its cumulative probability distribution (CDF) equals the distribution of the reference database provided by the BSR. Each climatological month results in one specific transformation to segregate the influence of seasonal variability. All transformations were developed at daily resolution as Eq. (1) described.

CMIP6 model	ID	CMIP6 model	ID	CMIP6 model	ID
ACCESS-CM2[250 km]	M01	ACCESS-ESM1-5 [250 km]	M02	AWI-CM-1-1-MR [100 km]	M03
BCC-CSM2-MR [100 km]	M04	CAMS-CSM1-0 [100 km]	M05	CAS-ESM2-0 [100 km]	M06
CESM2-WACCM [100 km]	M07	CIESM[100 km]	M08	CMCC-CM2-SR5 [100 km]	M09
CMCC-ESM2 [100 km]	M10	CNRM-CM6-1-HR [50 km]	M11	CNRM-CM6-1 [250 km]	M12
CNRM-ESM2-1 [250 km]	M13	EC-Earth3-CC [100 km]	M14	EC-Earth3-Veg-LR [250 km]	M15
EC-Earth3-Veg[100 km]	M16	EC-Earth3 [100 km]	M17	FGOALS-f3-L [100 km]	M18
FGOALS-g3 [250 km]	M19	FIO-ESM-2-0 [100 km]	M20	GFDL-CM4 [100 km]	M21
GFDL-ESM4 [100 km]	M22	GISS-E2-1-G [250 km]	M23	GISS-E2-1-H [250 km]	M24
HadGEM3-GC31 [250 km]	M25	IITM-ESM [100 km]	M26	INM-CM4-8 [100 km]	M27
INM-CM5-0 [100 km]	M28	IPSL-CM6A-LR [250 km]	M29	KACE-1-0-G [250 km]	M30
KIOST-ESM [250 km]	M31	MIROC6 [250 km]	M32	MPI-ESM1-2-HR [100 km]	M33
MPI-ESM1-2-LR [100 km]	M34	MRI-ESM2-0 [100 km]	M35	NESM3 [250 km]	M36
NorESM2-LM [250 km]	M37	NorESM2-MM [100 km]	M38	TaiESM1 [100 km]	M39
UKESM1-0-LL [250 km]	M40				

Table 2. CMIP6 models used in the study and their respective spatial resolution (sorted in alphabetical order).

$$SSR_{ERA5_{QM},t,s} = CDF^{-1}_{BSR,s}\Big[eCDF_{ERA5,s}\Big(SSR_{ERA5,t,s}\Big)\Big] \quad (1)$$

where t and s represent the day and the grid point for each climatological month. Figure S1 shows the SSR mapping using ERA5 database and the bias-corrected ERA5 dataset $SSR_{ERA5_{QM}}$

Performance evaluation of CMIP6 climate models

CMIP6 models were evaluated concerning their ability to represent the SSR's spatial variability and intra-annual seasonality during the historical timeframe. Figure 2 shows the three target areas used to investigate the models' performance, comprising regions of interest for the Brazilian solar energy sector:

- Area A1 includes the semi-arid region in the Brazilian Northeast with the highest surface solar irradiation and the lowest seasonal variability[40];
- Area A2 comprises the Southern region of Brazil, where the solar energy resource has the highest seasonal variability but presents a high demand for distributed PV systems and could take advantage of hybrid Wind-PV systems due to the high wind speed in the region[28];
- Area A3 covers the region that combines two advantages: a high surface solar irradiation and proximity to the main electricity consumer centers with fair coverage of the Brazilian interconnected electricity distribution system (SIN).Sixteen of the forty CMIP6 models provide SSR with a 250 km horizontal resolution, while only one offers a 50 km resolution. Before evaluation, all CMIP6 models were downscaled (bilinear approach) to the same horizontal resolution of the $ERA5_{QM}$ grid (around 27 km). The interpolation procedure was essential for a fair and unbiased comparison of the GCM models' achievements.

The performance evaluation was accomplished at the intersection between the ERA5 and CMIP6 databases (1980-2014). As discussed by[51], both temporal and spatial statistical performances were evaluated for the three target areas based on the following metrics:

- Spatial correlation (Rs): the Pearson correlation was calculated using the monthly average surface solar irradiation data from each grid point of the climate model (SSR_{Mx}), where Mx is the ID used for CMIP6 models listed in Table 2 and $ERA5_{QM}$ ($SSR_{ERA5_{QM}}$);
- Seasonal correlation (Rt): the Pearson correlation index was obtained from the SSR_{Mx} and $SSR_{ERA5_{QM}}$ time series of the monthly climatological averages (Jan to Dec);
- $uRMSD$: the unbiased root of mean squared deviations between the SSR_{Mx} and $SSR_{ERA5_{QM}}$ monthly climatological averages;
- SD ratio: the average value of the ratio between SSR_{Mx} and $SSR_{ERA5_{QM}}$ standard deviations in all three target areas.The statistically significant spatial correlation Rs (p-value < 0.05) demonstrates the skill of CMIP6 models in representing the mean spatial patterns of the SSR in the three target areas. In this sense, we select a subset of CMIP6 models with a significant spatial correlation for all twelve months in the three target areas.

The Taylor diagram was constructed using three metrics (Rt, $uRMSD$, and SD ratio) to assess how well the SSR data from CMIP6 models align with the SSR climatology of the $ERA5_{QM}$. By employing the Taylor Skill Score (TSS) approach[52], we utilized Eq. (2) to combine these metrics and identify the CMIP6 models that best represent the SSR climatology in the three regions of interest.

$$TSS = \frac{4\big(1+R_t\big)^4}{\big(f\sigma_{Mx}+1/f\sigma_{Mx}\big)^2\big(1+R_{t0}\big)^4} \quad (2)$$

where $f\sigma_{Mx}$ is the ratio between the variance of the CMIP6 model (Mx) and the variance of $ERA5_{QM}$, and R_{t0} is the maximum correlation attainable. According to this approach, a TSS value closer to unity indicates better performance of the model in representing the SSR climatology. Equation (2) yields a value of 1.0 as the climate model variance approaches the ERA_{QM} variance (i.e., $f\sigma_{Mx}$ tends to 1) and R tends to R_{t0}. On the contrary, TSS decreases towards zero as the correlation becomes increasingly negative or the model variance approaches zero or infinity. For fixed variance, skill increases linearly with correlation.

The CMIP6 models achieving TSS greater than 0.9 were combined to create a Smart Model Ensemble (SME) used to provide the SSR data for future climate scenarios. Similarly, the multi-model ensemble (ENS) was fetched by averaging the SSR_{Mx} data provided by each of the forty CMIP6 models. The individual model's assessment for comparison included the SME and ENS performances.

Assessment of impacts

The "climate change factor" approach proposed by Ref.[53] was adopted to assess the impacts of future climate pathways SSP2-4.5 e SSP5-8.5. The climate change factor (CCF) represents the percentage change in SSR in future scenarios over the model's prediction for the historical timeslice (1980-2014). This approach assumes that the model bias is preserved along the simulations, dismissing the need for bias corrections to evaluate the climate change signal. Equations (3) and (4) were used to estimate, respectively, the CCF and future SSR in each timeslice based on the truth reference ($ERA5_{QM}$). This approach was performed for each climatological month to produce future climatologies of CCF over SSR.

$$CCF_{Mx}\Big(geo, m, SSP, tslice\Big) = \frac{SSR_{Mx}\Big(geo, m, SSP, tslice\Big) - SSR_{Mx}\Big(geo, m, hist\Big)}{SSR_{Mx}\Big(geo, m, hist\Big)} \quad (3)$$

$$SSR\Big(geo, m, SSP, tslice\Big) = SSR_{ERA5_{QM}}\Big(geo, m\Big) + CCF_{Mx}\Big(geo, m, SSP, tslice\Big).SSR_{Mx}\Big(geo, m, hist\Big) \quad (4)$$

where the subscript Mx represents a specific CMIP6 model or ensemble, $tslice$, and $hist$ concerns the modelÂ´s outcomes for future and historical data frames. The CCF depends on the geographical location $geo = [lat, lon]$, and the month represented by m. The SSP is one of the future pathways for climate change (SSP2-4.5 or SSP5-8.5).

Data availability

This manuscript includes supplementary tables and figures to complement the information and results presented in the submitted paper. Results, additional datasets, and codes used in data analysis are deposited for public access at https://figshare.com/s/bc57a485308cbf01ea29 and https://figshare.com/s/22cccad668c8e3872254.

Received: 10 April 2024; Accepted: 20 September 2024
Published online: 21 October 2024

References

1. Osman, A. I. *et al.* Cost, environmental impact, and resilience of renewable energy under a changing climate: a review. *Environ. Chem. Lett.* **21**, 741–764. https://doi.org/10.1007/s10311-022-01532-8 (2023).
2. Gernaat, D. E. H. J. *et al.* Climate change impacts on renewable energy supply. *Nat. Clim. Change* **11**, 119–125. https://doi.org/10.1038/s41558-020-00949-9 (2021).
3. Bloomfield, H. *et al.* Quantifying the sensitivity of European power systems to energy scenarios and climate change projections. *Renew. Energy* **164**, 1062–1075. https://doi.org/10.1016/j.renene.2020.09.125 (2021).
4. Solaun, K. & Cerdá, E. Climate change impacts on renewable energy generation. A review of quantitative projections. *Renew. Sustain. Energy Rev.* **116**, 109415. https://doi.org/10.1016/j.rser.2019.109415 (2019).
5. Huber, I. *et al.* Do climate models project changes in solar resources?. *Sol. Energy* **129**, 65–84. https://doi.org/10.1016/j.solener.2015.12.016 (2016).
6. Wild, M., Folini, D., Henschel, F., Fischer, N. & Müller, B. Projections of long-term changes in solar radiation based on cmip5 climate models and their influence on energy yields of photovoltaic systems. *Sol. Energy* **116**, 12–24. https://doi.org/10.1016/j.solener.2015.03.039 (2015).
7. Pereira, E. B., Martins, F. R., Pes, M. P., da Cruz Segundo, E. I. & de A. Lyra, A. The impacts of global climate changes on the wind power density in brazil. *Renew. Energy* **49**, 107–110, https://doi.org/10.1016/j.renene.2012.01.053 (2013). Selected papers from World Renewable Energy Congress - XI.
8. Ha, S., Zhou, Z., Im, E.-S. & Lee, Y.-M. Comparative assessment of future solar power potential based on cmip5 and cmip6 multi-model ensembles. *Renew. Energy* **206**, 324–335. https://doi.org/10.1016/j.renene.2023.02.039 (2023).
9. Hou, X., Wild, M., Folini, D., Kazadzis, S. & Wohland, J. Climate change impacts on solar power generation and its spatial variability in Europe based on cmip6. *Earth Syst. Dyn.* **12**, 1099–1113. https://doi.org/10.5194/esd-12-1099-2021 (2021).
10. Dutta, R., Chanda, K. & Maity, R. Future of solar energy potential in a changing climate across the world: A cmip6 multi-model ensemble analysis. *Renew. Energy* **188**, 819–829. https://doi.org/10.1016/j.renene.2022.02.023 (2022).
11. Jerez, S. *et al.* The impact of climate change on photovoltaic power generation in Europe. *Nat. Commun.* **6**, 10014. https://doi.org/10.1038/ncomms10014 (2015).
12. Monerie, P.-A., Wainwright, C. M., Sidibe, M. & Akinsanola, A. A. Model uncertainties in climate change impacts on Sahel precipitation in ensembles of cmip5 and cmip6 simulations. *Clim. Dyn.* **55**, 1385–1401. https://doi.org/10.1007/s00382-020-05332-0 (2020).
13. ABSOLAR. Panorama da energia solar fotovoltaica no brasil e no mundo. Tech. Rep., Associação Brasileira de Energia Solar Fotovoltaica (2023).
14. EPE. Brazilian Energy Balance - Sumary Report,. *(Reference Year 2022) (Empresa de Pesquisas Energéticas* 2023 (Brazil, Ministério de Minas e Energia, 2023).
15. IRENA. Brazil energy profile. Tech. Rep., International Renewable Energy Agency (2022).
16. de Lima, F. J. L. *et al.* The seasonal variability and trends for the surface solar irradiation in northeastern region of Brazil. *Sustain. Energy Technol. Assess.* **35**, 335–346. https://doi.org/10.1016/j.seta.2019.08.006 (2019).
17. Santos, A. J. L. & Lucena, A. F. Climate change impact on the technical-economic potential for solar photovoltaic energy in the residential sector: a case study for brazil. *Energy Clim. Change* **2**, 100062. https://doi.org/10.1016/j.egycc.2021.100062 (2021).
18. de Jong, P. *et al.* Estimating the impact of climate change on wind and solar energy in brazil using a south American regional climate model. *Renew. Energy* **141**, 390–401. https://doi.org/10.1016/j.renene.2019.03.086 (2019).
19. Zuluaga, C. F., Avila-Diaz, A., Justino, F. B., Martins, F. R. & Ceron, W. L. The climate change perspective of photovoltaic power potential in Brazil. *Renew. Energy* **193**, 1019–1031. https://doi.org/10.1016/j.renene.2022.05.029 (2022).
20. Martins, F. R., Lima, F. J. L., Gonçalves, A. R., Costa, R. S. & Pereira, E. B. *Python Scripts for Data Analysis.*[SPACE]https://doi.org/10.6084/m9.figshare.25396210.v1 (2024).
21. Martins, F. R., Lima, F. J. L., Pereira, E. B., Costa, R. S. & Gonçalves, A. R. Research results - Climate change influence on surface solar irradiance. *figshare*[SPACE]https://doi.org/10.6084/m9.figshare.25396612.v1 (2024).
22. Firpo, M. A. F. *et al.* Assessment of cmip6 models' performance in simulating present-day climate in Brazil. *Front. Clim.*[SPACE]https://doi.org/10.3389/fclim.2022.948499 (2022).
23. Almazroui, M. *et al.* Assessment of cmip6 performance and projected temperature and precipitation changes over South America. *Earth Syst. Environ.* **5**, 155–183. https://doi.org/10.1007/s41748-021-00233-6 (2021).
24. Ortega, G., Arias, P. A., Villegas, J. C., Marquet, P. A. & Nobre, P. Present-day and future climate over central and South America according to cmip5/cmip6 models. *Int. J. Climatol.* **41**, 6713–6735. https://doi.org/10.1002/joc.7221 (2021).
25. Dantas, L. G., dos Santos, C. A. C., Santos, C. A. G., Martins, E. S. P. R. & Alves, L. M. Future changes in temperature and precipitation over Northeastern Brazil by cmip6 model. *Water*[SPACE]https://doi.org/10.3390/w14244118 (2022).
26. Hunt, J. . D., Stilpen, D. & de Freitas, M. . A. . V. A review of the causes, impacts and solutions for electricity supply crises in Brazil. *Renew. Sustain. Energy Rev.* **88**, 208–222. https://doi.org/10.1016/j.rser.2018.02.030 (2018).

27. Gonzalez, J. O. & Martins, F. R. Performance study of a photovoltaic system operating on the southeastern coast of Brazil. *IEEE Lat. Am. Trans.* **22**, 410–417. https://doi.org/10.5194/gmd-9-3461-2016 (2024).
28. Davis, N. N. *et al.* The global wind atlas: A high-resolution dataset of climatologies and associated web-based application. *Bull. Am. Meteor. Soc.* **104**, E1507–E1525. https://doi.org/10.1175/BAMS-D-21-0075.1 (2023).
29. Amarante, O. A. C., Brower, M., Zack, J. & Sá, A. L. *Atlas do Potencial Eólico Brasileiro*, 2nd edn (Centro de Pesquisas de Energia Elétrica, Ministério de Minas e Energia, Brazil, 2017).
30. Velloso, M. F. A., Martins, F. R. & Pereira, E. B. Case study for hybrid power generation combining hydro- and photovoltaic energy resources in the Brazilian semiarid region. *Clean Technol. Environ. Policy* **21**, 941–952. https://doi.org/10.1007/s10098-019-01685-1 (2019).
31. Ferraz de Campos, E. *et al.* Hybrid power generation for increasing water and energy securities during drought: Exploring local and regional effects in a semi-arid basin. *J. Environ. Manag.* **294**, 112989. https://doi.org/10.1016/j.jenvman.2021.112989 (2021).
32. Filippo Antoniolli, A., Naspolini, H. F., de Abreu, J. F. & Rüther, R. The role and benefits of residential rooftop photovoltaic prosumers in Brazil. *Renew. Energy* **187**, 204–222. https://doi.org/10.1016/j.renene.2022.01.072 (2022).
33. Beck, H. E. *et al.* Publisher correction: Present and future köppen-geiger climate classification maps at 1-km resolution. *Sci. Data* **7**, 274. https://doi.org/10.1038/s41597-020-00616-w (2020).
34. Avila-Diaz, A., Benezoli, V., Justino, F., Torres, R. & Wilson, A. Assessing current and future trends of climate extremes across Brazil based on reanalyses and earth system model projections. *Clim. Dyn.* **55**, 1403–1426. https://doi.org/10.1007/s00382-020-05333-z (2020).
35. Alvares, C. A., Stape, J. L., Sentelhas, P. C., de Moraes Gonçalves, J. L. & Sparovek, G. Koppen's climate classification map for Brazil. *Meteorol. Z.* **22**, 711–728. https://doi.org/10.1127/0941/2948/2013/0507 (2013).
36. Martins, F., Pereira, E., Silva, S., Abreu, S. & Colle, S. Solar energy scenarios in Brazil, part one: Resource assessment. *Energy Policy* **36**, 2853–2864. https://doi.org/10.1016/j.enpol.2008.02.014 (2008).
37. Casagrande, M. S. G. *et al.* Numerical assessment of downward incoming solar irradiance in smoke influenced regions'a case study in Brazilian amazon and cerrado. *Remote Sens.*[SPACE]https://doi.org/10.3390/rs13224527 (2021).
38. Sianturi, Y. & Marjuki Sartika, K. Evaluation of ERA5 and MERRA2 reanalyses to estimate solar irradiance using ground observations over Indonesia region. *AIP Conf. Proc.* **2223**, 020002. https://doi.org/10.1063/5.0000854 (2020).
39. Boilley, A. & Wald, L. Comparison between meteorological re-analyses from era-interim and merra and measurements of daily solar irradiation at surface. *Renew. Energy* **75**, 135–143. https://doi.org/10.1016/j.renene.2014.09.042 (2015).
40. Pereira, E. B. *et al.Brazilian Atlas for Solar Energy*, 2nd edn (Instituto Nacional de Pesquisas Espaciais, Ministério de Ciência, Tecnologia e Inovação, Brazil, 2017).
41. Hersbach, H. *et al.* The era5 global reanalysis. *Q. J. R. Meteorol. Soc.* **146**, 1999–2049. https://doi.org/10.1002/qj.3803 (2020).
42. Urraca, R. *et al.* Evaluation of global horizontal irradiance estimates from era5 and cosmo-rea6 reanalyses using ground and satellite-based data. *Sol. Energy* **164**, 339–354. https://doi.org/10.1016/j.solener.2018.02.059 (2018).
43. Eyring, V. *et al.* Overview of the coupled model intercomparison project phase 6 (cmip6) experimental design and organization. *Geosci. Model Dev.* **9**, 1937–1958. https://doi.org/10.5194/gmd-9-1937-2016 (2016).
44. O'Neill, B. C. *et al.* The scenario model intercomparison project (scenariomip) for cmip6. *Geosci. Model Dev.* **9**, 3461–3482. https://doi.org/10.5194/gmd-9-3461-2016 (2016).
45. Riahi, K. *et al.* The shared socioeconomic pathways and their energy, land use, and greenhouse gas emissions implications: An overview. *Glob. Environ. Change* **42**, 153–168. https://doi.org/10.1016/j.gloenvcha.2016.05.009 (2017).
46. Jr, R. P., Burgess, M. G. & Ritchie, J. Plausible 2005–2050 emissions scenarios project between 2°c and 3°c of warming by 2100. *Environ. Res. Lett.* **17**, 024027. https://doi.org/10.1088/1748-9326/ac4ebf (2022).
47. Gidden, M. J. *et al.* Global emissions pathways under different socioeconomic scenarios for use in cmip6: a dataset of harmonized emissions trajectories through the end of the century. *Geosci. Model Dev.* **12**, 1443–1475. https://doi.org/10.5194/gmd-12-1443-2019 (2019).
48. Dellink, R., Chateau, J., Lanzi, E. & Magné, B. Long-term economic growth projections in the shared socioeconomic pathways. *Glob. Environ. Change* **42**, 200–214. https://doi.org/10.1016/j.gloenvcha.2015.06.004 (2017).
49. Rajczak, J., Kotlarski, S. & Schär, C. Does quantile mapping of simulated precipitation correct for biases in transition probabilities and spell lengths?. *J. Clim.* **29**, 1605–1615. https://doi.org/10.1175/JCLI-D-15-0162.1 (2016).
50. Boé, J., Terray, L., Habets, F. & Martin, E. Statistical and dynamical downscaling of the seine basin climate for hydro-meteorological studies. *Int. J. Climatol.* **27**, 1643–1655. https://doi.org/10.1002/joc.1602 (2007).
51. Lauer, A. *et al.* Benchmarking cmip5 models with a subset of esa cci phase 2 data using the esmvaltool. *Remote Sensing of Environment* **203**, 9–39, https://doi.org/10.1016/j.rse.2017.01.007 (2017). Earth Observation of Essential Climate Variables.
52. Taylor, K. E. Summarizing multiple aspects of model performance in a single diagram. *J. Geophys. Res. Atmos.* **106**, 7183–7192. https://doi.org/10.1029/2000JD900719 (2001).
53. Navarro-Racines, C. E., Tarapues-Montenegro, J. E. & Ramírez-Villegas, J. A. Bias-correction in the ccafs-climate portal: A description of methodologies. decision and policy analysis (dapa) research area. Tech. Rep., International Center for Tropical Agriculture (CIAT), Cali, Colômbia (2000).

Acknowledgements

The authors thank DIIAV/INPE and Unifesp for their institutional support. Thanks to CNPq for the research scholarships to Fernando Martins, José Orsini and Enio Pereira. The authors also thanks to National Institute of Science and Technology for Climate Change - INCT-MC Project Phase 2 (Grants FAPESP 2014/50848-9, CNPq 465501/2014-1, and CAPES/FAPS No 16/2014).

Author contributions

Conceptualization and investigation: F.J.L.L., A.R.G., R.S.C., and F.R.M.; methodology: F.J.L.L, A.R.G., R.S.C., and F.R.M.; code developments: F.J.L.L, M.P.P.; data analysis: F.J.L.L., R.S.C., A.R.G., and F.R.M.; writing-original draft preparation: F.J.L.L., A.R.G., R.S.C., A.P.P.S. and F.R.M.; writing-review and editing: F.J.L.L., A.R.G., R.S.C. and F.R.M.; funding acquisition: J.A.M.O., E.B.P., and F.R.M. All authors reviewed the manuscript.

Declarations

Competing interests

The authors declare no competing interests.

Additional information

Supplementary Information The online version contains supplementary material available at https://doi.

org/10.1038/s41598-024-73769-y.

Correspondence and requests for materials should be addressed to F.R.M.